Astron. Astrophys. 271, 65–70 (1993)

ASTRONOMY
AND
ASTROPHYSICS

The superluminal character of the compact steep spectrum quasar 3C 216

T. Venturi[1,2], T.J. Pearson[2], P.D. Barthel[3], and T. Herbig[2]

[1] Istituto di Radioastronomia, Via Irnerio, 46, I-40126 Bologna, Italy
[2] California Institute of Technology, 105-24, Pasadena, CA 91125, USA
[3] Kapteyn Astronomical Institute, P.O. Box 800, NL-9700 AV Groningen, The Netherlands

Received January 18, accepted August 8, 1992

Abstract. We report the results of fourth epoch VLBI observations at 4990.99 MHz, with a resolution of ~ 1 mas, of the compact steep-spectrum quasar 3C 216. Superluminal motion in this object is confirmed. Although a constant superluminal expansion at $v_{app} = 3.9c \pm 0.6$ is not ruled out, our four epoch data are suggestive of component deceleration.

In this paper we discuss the possibility of deceleration taking into account the compact steep spectrum nature of this quasar.

We conclude that (a) compact steep spectrum sources may show the same beaming and orientation phenomena as extended sources and (b) the compact steep spectrum nature of the source could offer an explanation for the possible deceleration.

Key words: quasars – radio – superluminal motion

1. Status of the radio and optical observations of 3C 216

3C 216 is a compact steep-spectrum (CSS) radio source associated with a quasar at a redshift of 0.668 (Pearson & Readhead 1988, and references therein). The overall spectrum of the source at radio frequencies is unusual among CSS sources: it is steep up to ~ 10 GHz, but then it flattens out at higher frequencies ($\alpha \sim 0.3$ for $\nu \geq 10$ GHz, see Herbig & Readhead 1992, and references therein). It is one of the very few CSS sources for which superluminal motion has been detected (other cases are 3C 147, Alef et al. 1990, and 3C 380, Wilkinson 1990), although few such sources have been monitored closely. Barthel et al. (1988; hereafter BPR88) reported superluminal motion in 3C 216 on the basis of observations at 4990.99 MHz at three epochs. In this paper we present the results of a fourth epoch observation. We assume $H_0 = 100\,\mathrm{km\,s^{-1}\,Mpc^{-1}}$ and $q_0 = 0.5$ throughout the paper. At the distance of 3C 216 ($z = 0.668$) 1 mas corresponds to 3.6 pc.

The radio source 3C 216 has a core-dominated triple structure with an overall angular size of 2.5 arcsec (Pearson et al. 1985) which is embedded in a low-brightness halo extending ~ 8 arcsec (BPR88). On milliarcsecond scales, 3C 216 displays a core-jet morphology, in which jet components appear to move away from the (assumed stationary) core (BPR88). The milliarcsecond-scale jet, in *p.a. 153°*, is approximately perpendicular to the axis of the arcsecond-scale triple structure. Lower-resolution VLBI observations at 1.6 and 0.6 GHz with resolutions of ~ 30 mas (Fejes et al. 1992) show that the jet extends southwards to a distance of 140 mas (0.5 kpc) from the most compact nuclear component, where it bends abruptly by almost 90° towards east. In common with many CSS sources, 3C 216 has a high intrinsic rotation measure: $\mathrm{RM} = 1386\,\mathrm{rad\,m^{-2}}$ (Tabara & Inoue 1980). This suggests that the associated quasar has a dense nuclear environment, which should be taken into account when discussing the nature and the observed properties of the radio source.

On the basis of its optical variability and high polarization ($p = 21\%$), 3C 216 was classified as a blazar by Angel & Stockman (1980). High optical polarisation was confirmed by Impey & Tapia (1990) and Impey et al. (1991), who found a polarisation degree of $p = 3.8 \pm 0.2\%$. Impey et al. (1991) found that those sources with the highest optical polarisation show a strong misalignment at radio frequencies between the position angle of the milliarcsecond (VLBI) and arcsecond structure, θ_{VLBI} and θ_{ext} respectively. This is indeed the case of 3C 216, for which the misalignment is $\Delta\theta = 108°$ (BPR88). The optical polarisation vector in 3C 216 is almost aligned with the arcsecond (VLA) radio structure.

3C 216 is unique in showing both blazar and CSS characteristics. In order to investigate this dual character we have continued to monitor the structural evolution of 3C 216. Results of this monitoring program are presented here.

2. Observations and data reduction

We observed 3C 216 at 4990.99 MHz in 1988.19 for 6 h with a global VLBI array consisting of 10 antennas: Effels-

Send offprint requests to: T. Venturi (Bologna)

berg, Westerbork, Onsala, Jodrell Bank Mk-2, Medicina, Haystack, Green Bank, Iowa, VLA phased array, and Owens Valley. The resolution provided by this array is 2.5 x 0.7 mas. We used the Mark-II recording system, and correlated the data using the 16-station JPL/Caltech Block II correlator. The correlated data were fringe fitted using the standard NRAO AIPS program CALIB; subsequent analysis was carried out using programs in the Caltech VLBI Package (Pearson 1991).

We obtained a starting model for the self-calibration by fitting a Gaussian model to the measured amplitudes and closure phases. The model consists of four components: the strongest, containing almost 70% of the total flux density, is assumed to be the stationary component in the previous maps (see BPR88); two components are aligned in position angle $\sim 152°$, and a fourth, more diffuse component is located further away, at $\sim$ 6 mas, in *p.a.* $\sim 135°$. Starting from this model, we obtained a satisfactory image after five iterations of self-calibration. Gain corrections were smaller than 5% for each antenna. The final image, shown in Fig. 1, is convolved with a circular Gaussian beam of FWHM 1.2 mas. The noise in this image is 0.7 mJy per beam, the total flux density is 625 mJy, and the peak flux density is 435 mJy per beam. The flux density in the core and in component A is 566 mJy ($\sim$91% of the total), while the flux density in components B and C is 42 and 17 mJy respectively. These values were derived by means of the program IMFIT in AIPS.

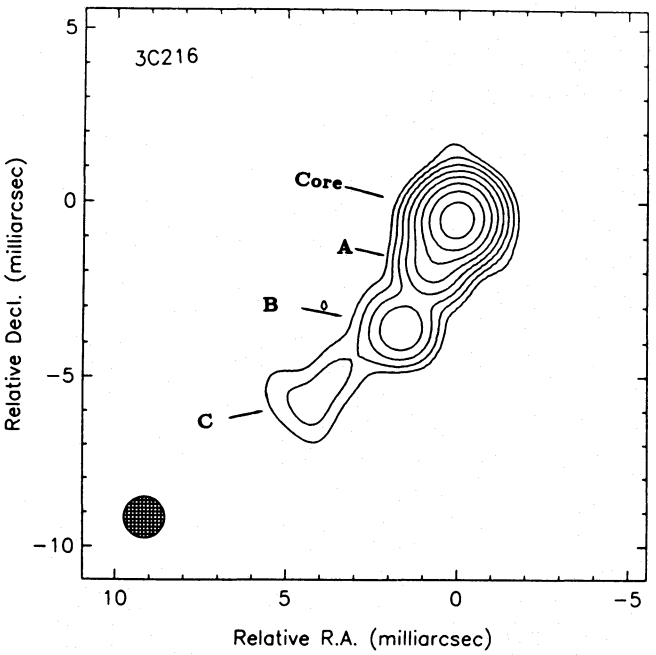

Fig. 1. Contour plot of the fourth epoch VLBI map of 3C 216 at 4990.99 MHz. The peak flux density is 0.45 Jy per beam. Levels are: −0.5, 0.5, 1, 2, 4, 8, 16, 32, 64% of the peak. The map is restored with a round Gaussian beam of 1.2 mas, plotted in the bottom left corner

3. The structural evolution of 3C 216

The parsec-scale morphology of 3C 216 is typical of one-sided core-jet radio sources. The northernmost of the four components is the brightest and most compact and is assumed to be the core (this assumption needs confirmation with radio spectral data). In Table 1 we report the positions of the various components with respect to the core (assumed stationary). The jet has a position angle $\sim 153°$; we have divided it into 3 components labelled A, B, C (Fig. 1 and Table 1). Component A lies 1.42 mas ($\sim$ 5 pc) from the core. Component B, at $\sim$ 13 pc, was found to be superluminal on the basis of the first three epochs (BPR88). Component C, at about 5 mas (17 pc) from the core, has a different position angle $\sim 143°$, suggesting that the jet bends towards the east.

In order to determine the relative positions of the components and hence their apparent velocities we adopted the following procedure. We estimated the locations and sizes of the components from the brightness peaks in the image, and then refined these values by least-squares fits of elliptical Gaussian components to the final self-calibrated visibilities (Table 1). We estimate the uncertainty in the location of components A and B as 10% of the beam width, i.e. 0.1 mas.

Table 1. Distance in milliarcsecond and position angle of the components A, B and C with respect to the core for all four epochs. The values with * are taken by BPR88. The others are the results of the analysis described in the present paper

Epoch	A		B		C	
	r (mas)	P.A. (°)	*r* (mas)	P.A. (°)	*r* (mas)	P.A. (°)
1979.92	—		1.88±0.10*	155	—	
1984.40	1.47±0.10	151	3.04±0.10*	153	6.25±0.20	143
1986.42	1.55±0.10	153	3.39±0.10*	153	6.02±0.20	142
1988.19	1.42±0.10	151	3.60±0.10	153	5.82±0.20	143

Component C is more diffuse and has a lower surface brightness, so the determination of the peak is more uncertain. The uncertainty we estimate for the location of its position is 0.2 mas. Although there are small differences between the images, we cannot conclude that the overall morphology and total flux density of this component have changed significantly between 1986.42 and 1988.19. Any change in the position of this component is small compared to its extent.

The positional accuracy of components A and B in the

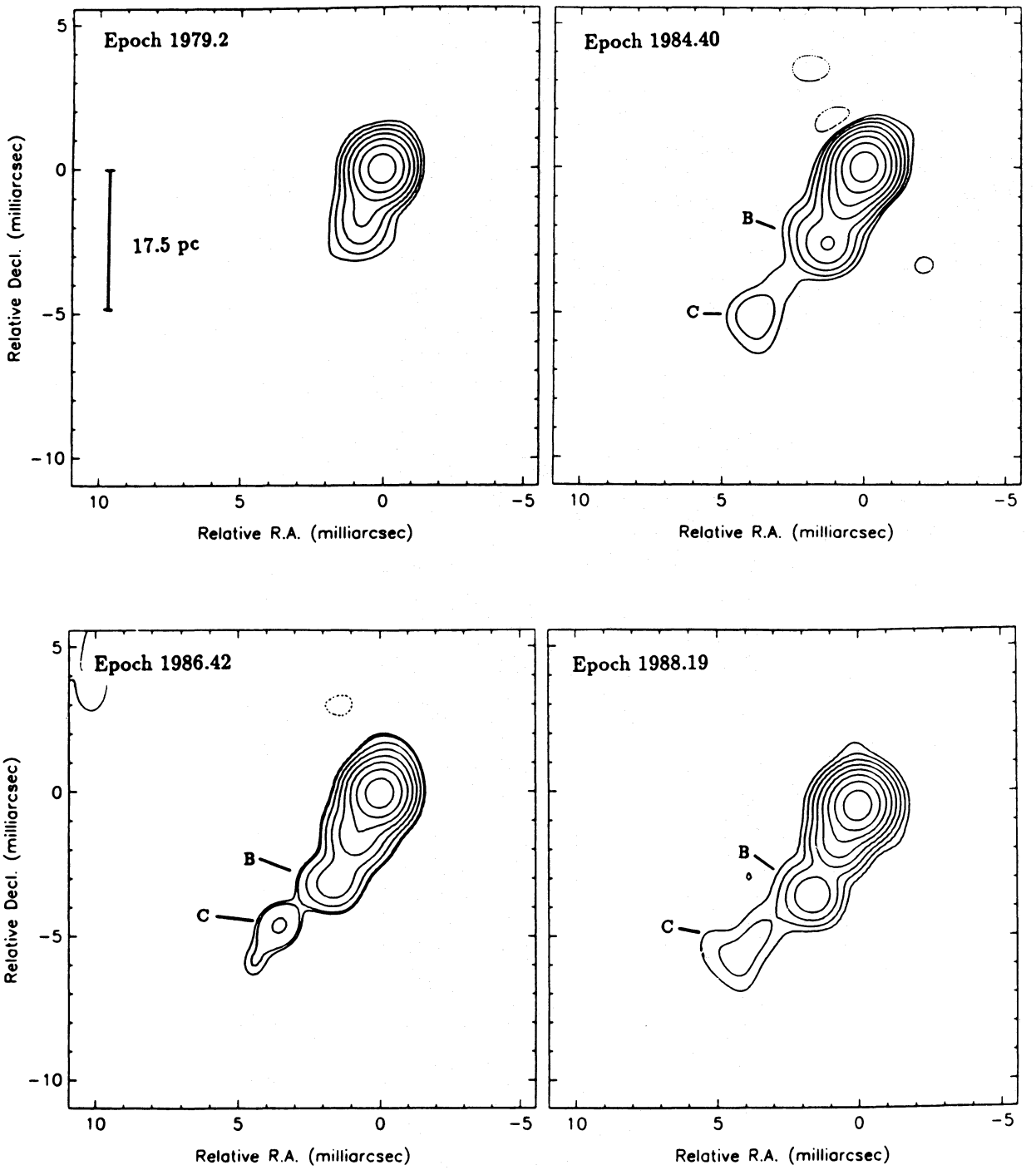

Fig. 2. Contour plots of all four epoch VLBI maps of 3C 216 at 4990.99 GHz. Each map is convolved with a round Gaussian beam with FWHM = 1.2 mas. (a) 1979.92. The peak flux density is 0.81 Jy per beam; levels are: −1, 1, 2, 4, 8, 16, 32, 64% of the peak. (b) 1984.40. The peak flux density is 0.50 Jy per beam; levels are: −0.5, 0.5, 1, 2, 4, 8, 16, 32, 64% of the peak. (c) 1986.42. The peak flux density is 0.50 Jy per beam; levels are: −0.8, 0.8, 1, 2, 4, 8, 16, 32, 64% of the peak. (d) 1988.19. The peak flux density is 0.45 Jy per beam; levels are: −0.5, 0.5, 1, 1, 2, 4, 8, 16, 32, 64% of the peak

first 3 epochs was examined by careful remapping of these older data sets, following the same procedure described in Sect. 2 and par. 3.1 for the 4th data set. The positions we obtained agree within the errors with those published in BPR88. This further check confirms the significance of the errors on those positions. For a straightforward comparison of the 1988.19 map with the older ones, in Fig. 2 we show the final maps obtained from our reanalysis of all data sets. Each map is convolved with a round Gaussian beam with FWHM = 1.2 mas. In Table 1 the positions of components A, B and C in all three previous epochs are also given.

Component A is also present in the second and third epoch (BPR88), but it was not visible in 1979.92. A fit of this component shows that its position has remained constant within the errors from 1984.40 to 1988.19.

Comparison of the position of component B at 1988.19 and at 1986.42 (BPR88) leads to a proper motion relative to the core of $\mu = 0.12 \pm 0.03$ mas yr^{-1} which implies $\beta_{app} = 2.6 \pm 0.7$.

4. Discussion

The result from our fourth epoch observation confirms the superluminal character of 3C 216.

The expansion velocity we derive for component B between 1986.42 and 1988.19, $\beta_{app} = 2.6$, is smaller almost by a factor of two than that derived by BPR88, even allowing for the estimated errors.

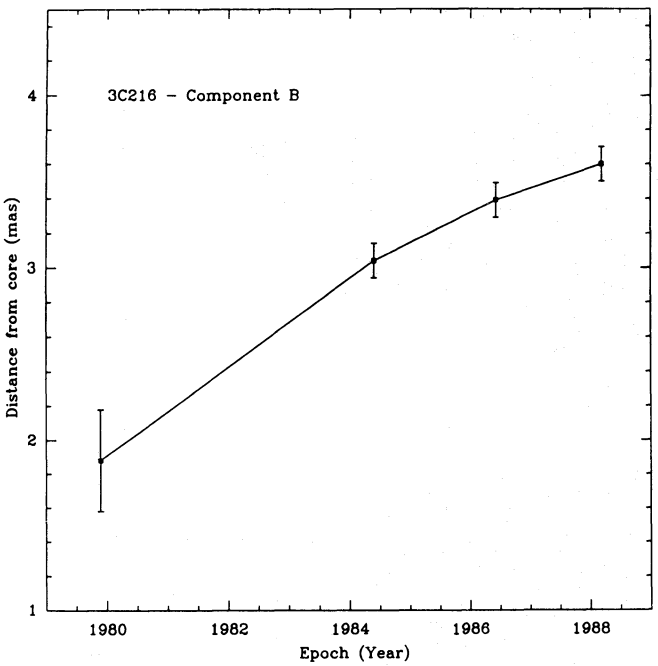

Fig. 3. Distance of component B in milliarcseconds (Y axis) versus epoch (X axis). Data on the first three epochs are taken from BPR88

In Fig. 3 we plot the distance d of component B from the core versus time t. The large error in the first epoch measurement makes it possible to fit all four data points with one straight line. A weighted least-square fit on all epochs gives an apparent proper motion $\mu = 0.18 \pm 0.03$ mas yr^{-1}, which corresponds to $\beta_{app} = 3.9 \pm 0.6$. This value is lower than the one derived in BPR88, but still in agreement with it if we allow for the uncertainty in the derived values. It is worth noticing, however, that the velocity v_{app} derived from epochs 3 and 4 here would be in very good agreement with the position of component B in epoch 2, too, but in this case the component should have been easily visible in the first-epoch image at 2.3 mas from the core.

It is not implausible that the component we see in 1979.92 is actually a blending of A and B, not resolved by those observations. If this were the case, the position derived in BPR88 would be the barycenter of A and B. We therefore cannot exclude that in 1979.92 component B was located in a position consistent with the expansion velocity derived on the basis of the fourth epoch observations. In such a frame the nature of 3C 216 would be quite interesting, since the radio structure would be stationary within the first ~ 2 mas (~ 7.2 pc) from the peak, with a superluminal component ($\beta_{app} = 2.6$) appearing beyond this distance.

Another possibility suggested by our new data is that the speed of this component has decreased, whereas its direction has remained constant. The monitoring of many superluminal sources in the past decade has shown that the velocity vector of brightness features is not always constant. In 3C 345, for example, different components appear to move along different paths and their speeds also differ (Zensus 1990); in 4C 39.25 a superluminal component is located between two stationary features and its velocity is suspected to be decreasing in time (Marcaide et al. 1990); a large fraction of the S5-survey radio sources displays different component velocities or stationary features (Witzel et al. 1988: Schalinski 1990).

Single dish monitoring of this source at various frequencies shows that the total flux density of the source had a maximum around 1980, and that it has been almost constant since 1985 (Hugh & Margo Aller, private communication). The decrease from the peak flux density was larger at higher frequencies. If we believe that a burst of radio emission in variable radio sources is related to the birth of a new component, we may explain the morphological changes and flux variability from 1979.92 in 3C 216 with the birth of component B.

A change in apparent velocity, β_{app}, could be due to either a change in the bulk flow Lorentz factor, γ, a change in the angle to the line of sight, θ, or a combination of the two. From the measured values of β_{app} in 3C 216, 4.7 (between 1979.92 and 1986.42) and 2.6 (between 1986.42 and 1988.19), constraints may be placed on the changes in γ and θ, as shown in Fig. 4. For example, if θ remained

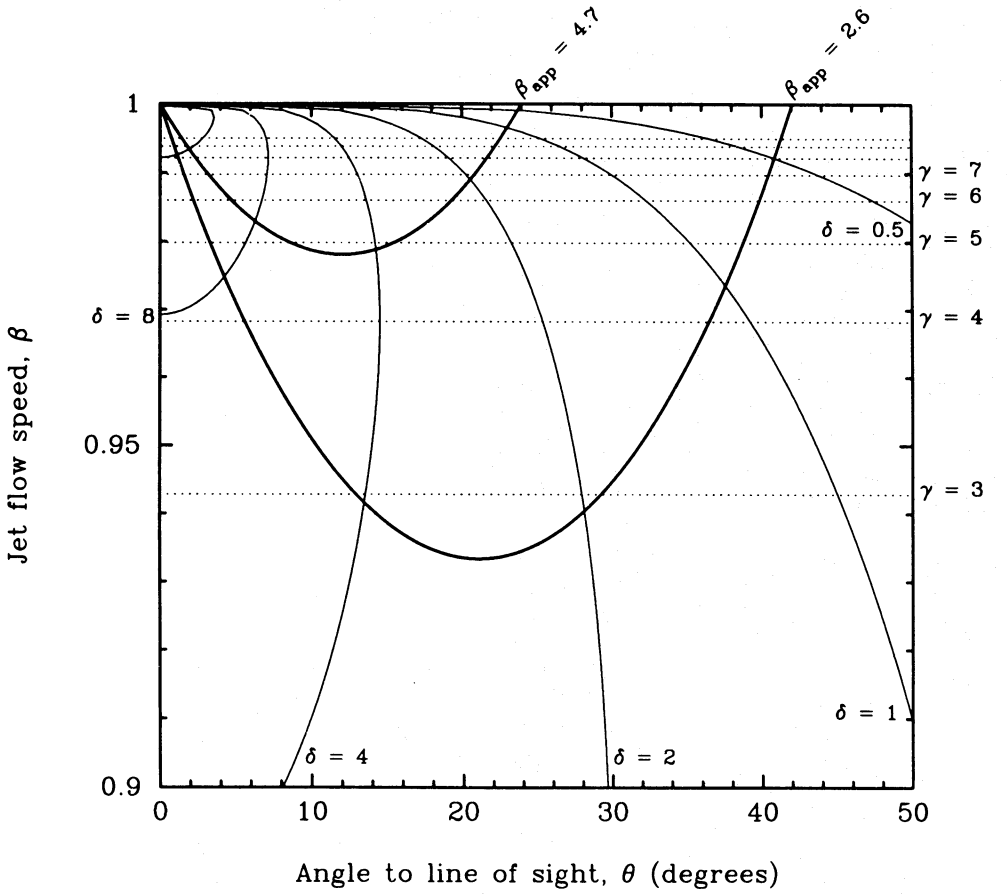

Fig. 4. Dependence of the apparent speed of the superluminal component on the angle to the line of sight, θ, and the intrinsic flow velocity, β. *Heavy lines* show the loci on which the component is constrained by the measured apparent speed, β_{app}, for two values of β_{app}. The *horizontal dotted lines* show the Lorentz factor γ corresponding to β. The *light lines* are loci of constant Doppler factor $\delta=[\gamma(1-\beta\cos\theta)]^{-1}$ for $\delta=0.5, 1, 2, 4, 8, 16$

constant (vertical line in Fig. 3), then θ must be less than 24° (BPR88) and there must have been a substantial reduction in γ unless the jet lies very close to the line of sight. On the other hand, if γ remained constant (horizontal line in Fig. 4), then γ must be greater than 4.8 (BPR88) and the angle to the line of sight has either increased by $\sim 20°$ (if the original angle was $>12°$), or decreased by a small amount if the original angle was $<12°$.

A change in either γ or θ would cause a change in the apparent brightness of the jet component. The brightness changes by some power (~ 3) of the Doppler factor $\delta=\gamma^{-1}(1-\beta\cos\theta)^{-1}$. The flux density of the superluminal component B was observed to change by less than 10%, which suggests that there was little change in δ. From Fig. 4 we can see that this requires that the Lorentz factor γ changed rather than the angle to the line of sight θ. For example, if $\theta\approx 20°$ and γ decreased from ~ 5 to ~ 3, little change in the Doppler factor would have occurred. Alternatively, the Doppler factor, which is related to the bulk flow speed of the emitting material, may be unrelated to the "pattern" speed measured in the VLBI observations; in this case we cannot distinguish between changes in θ and γ.

The presumed deceleration may be due to interaction of the radio jet in 3C 216 with an external medium. Other radio properties of 3C 216 support the idea that this quasar contains a dense interstellar medium. First of all it is a compact steep-spectrum source. Even though the nature of CSS sources is far from being understood, one plausible explanation for their observed distorted radio morphologies is interaction between their radio jets and a dense external medium (e.g. Fanti et al. 1990). Furthermore, its large intrinsic rotation measure supports the existence of a dense medium.

Our observations thus suggest that the blazar properties of 3C 216 are due to its favourable orientation relative to the line of sight and that its compact steep-spectrum properties are due to interaction of the jet with a dense interstellar medium. This leads to the conclusion that compact steep-spectrum objects, which have been shown to be intrinsically small sources (Fanti et al. 1985), may show a similar dependence of their properties on orientation as do the extended steep-spectrum sources.

New forthcoming 4990.99 MHz observations of our monitoring program on this source will enable us to discriminate among the possible scenarios we took into account.

Acknowledgments. We are grateful to the U.S. and European VLBI networks for allocating observing time for these observations, and Margo and Hugh Aller for providing their flux-density monitoring data in advance of publication. We thank

Prof. R. and C. Fanti and Dr. F. Mantovani for comments and suggestions on the manuscript. The work was supported in part by NSF grant AST-8814554 and by the CNR NATO fellowship 203.02.19. TJP is grateful for the hospitality of the Kapteyn Laboratory, Groningen, and thanks the Netherlands Organization for Pure Research for a Visitor Grant.

References

Alef W., Preuss E., Kellermann K.I., 1990, in: Fanti C., Fanti R., O'Dea C.P., Schilizzi R.T. (eds.) Compact Steep-Spectrum and GHz-Peaked Spectrum Radio Sources. Consiglio Nazionale delle Ricerche, Istituto di Radioastronomia, Bologna, p. 149

Angel J.R.P., Stockman H.S., 1980, ARA&A 18, 321

Barthel P.D., Pearson T.J., Readhead A.C.S., 1988, ApJ 329, L51 (BPR88)

Fanti C., Fanti R., Parma P., Schilizzi R.T., van Breugel W.J.M., 1985, A&A 143, 292

Fanti C., Fanti R., O'Dea C.P., Schilizzi R.T., 1990, in: Fanti C., Fanti R., O'Dea C.P., Schilizzi R.T. (eds.) Compact Steep-Spectrum and GHz-Peaked Spectrum Radio Sources. Consiglio Nazionale delle Ricerche, Istituto di Radioastronomia, Bologna

Fejes I., Porcas R.W., Akujor C.E., 1992, A&A 257, 459

Herbig T., Readhead A.C.S., 1992, ApJS 81, 83

Impey C.D., Tapia S., 1990, ApJ 354, 124

Impey C.D., Lawrence C.R., Tapia S., 1991, ApJ 375, 46

Marcaide J.M., Alberdi A., Elosegui P., Marscher A.P., Zhang Y.F., Shaffer D.B., Schalinski C.J., Witzel A., Jackson N., Sandell G., 1990, in: Zensus A., Pearson T.J. (eds.) Parsec-Scale Radio Jets. Cambridge University Press, Cambridge, p. 59

Pearson T.J., 1991, BAAS 23, 991

Pearson T.J., Readhead A.C.S., 1988, ApJ 328, 114

Pearson T.J., Perley R.A., Readhead A.C.S., 1985, AJ 90, 738

Schalinski C.J. 1990, Ph.D. Thesis, University of Bonn

Tabara H., Inoue M., 1980, A&AS 39, 379

Wilkinson P.N., 1990, in: Fanti C., Fanti R., O'Dea C.P., Schilizzi R.T. (eds.) Compact Steep-Spectrum and GHz-Peaked Spectrum Radio Sources. Consiglio Nazionale delle Ricerche, Istituto di Radioastronomia, Bologna, p. 115

Witzel A., Schalinski C.J., Johnston K.J., Biermann P.I., Krichbaum T.P., Hummel C.A., Eckart A., 1988, A&A 206, 245

Zensus J.A., 1990, in: Zensus A., Pearson T.J. (eds.) Parsec-Scale Radio Jets. Cambridge University Press, Cambridge, p. 28